DOI:10.1111/j.1600-0625.2008.00790.x
www.blackwellpublishing.com/EXD

Original Article

Astaxanthin, canthaxanthin and β-carotene differently affect UVA-induced oxidative damage and expression of oxidative stress-responsive enzymes

Emanuela Camera[1,2], Arianna Mastrofrancesco[1], Claudia Fabbri[1], Felicitas Daubrawa[2], Mauro Picardo[1], Helmut Sies[2] and Wilhelm Stahl[2]

[1]Laboratorio di Fisiopatologia Cutanea, Istituto Dermatologico San Gallicano (IRCCS), Rome, Italy;
[2]Institut für Biochemie und Molekularbiologie I, Heinrich Heine Universität, Düsseldorf, Germany
Correspondence: Emanuela Camera, Laboratorio di Fisiopatologia Cutanea, Istituto Dermatologico San Gallicano (IRCCS), Via Elio Chianesi 53, I-00128, Rome, Italy, Tel.: +39 (0)6 5266 6241, Fax: +39 (0)6 5266 6247, e-mail: camera@ifo.it

Accepted for publication 14 July 2008

Abstract: Carotenoids are used for systemic photoprotection in humans. Regarding mechanisms underlying photoprotective effects of carotenoids, here we compared the modulation of UVA-related injury by carotenoids. Human dermal fibroblasts (HDF) were exposed to moderate doses of UVA, which stimulated apoptosis, increased levels of reactive oxygen species and thiobarbituric acid reactive substances, decreased antioxidant enzymes activities, promoted membrane perturbation, and induced the expression of heme oxygenase-1 (HO-1). The carotenoids astaxanthin (AX), canthaxanthin (CX) and β-carotene (βC) were delivered to HDF 24 h before exposure to UVA. Astaxanthin exhibited a pronounced photoprotective effect and counteracted all of the above-mentioned UVA-induced alterations to a significant extent. β-Carotene only partially prevented the UVA-induced decline of catalase and superoxide dismutase activities, but it increased membrane damage and stimulated HO-1 expression. Moreover, βC dose-dependently induced caspase-3 activity following UVA exposure. In contrast, CX had no effect on oxidative damage, except for HO-1 expression, which was augmented. Uptake of AX by fibroblasts was higher than that of the other two carotenoids. The photostability of the three compounds in fibroblasts was AX > CX >> βC. The data indicate that the oxo-carotenoid AX has a superior preventive effect towards photo-oxidative changes in cell culture.

Key words: antioxidant enzymes – apoptosis – carotenes – skin photodamage – xanthophylls

Please cite this paper as: Astaxanthin, canthaxanthin and β-carotene differently affect UVA-induced oxidative damage and expression of oxidative stress-responsive enzymes. Experimental Dermatology 2008.

Introduction

Various types of skin damage are caused by exposure to UV light (1). UVA-induced damage is mainly mediated by reactive oxygen species (ROS) which are generated in photosensitising reactions (2,3). UVA triggers the generation of singlet oxygen ($^1O_2$) via photosensitisation, which activates a series of $^1O_2$-dependent cellular response pathways. The induction of matrix metalloproteinases along with the accumulation of the age-associated mtDNA deletions are typical $^1O_2$-mediated effects (4,5). The final consequences of UVA irradiation and exposure to $^1O_2$ are immunosuppressive reactions, photoaging, or photocarcinogenesis (6). UVA light is primarily involved in photoaccelerated skin aging, because it deeply penetrates the dermal layer, where fibroblasts prime aberrant extracellular matrix remodelling. Additionally, UVA-induced apoptosis is implicated in skin photoageing (7). UVA light depletes the antioxidant defense system of fibroblasts, especially affecting catalase (CAT) and superoxide dismutase (SOD) (8). Supplementation with antioxidants may reinforce the endogenous defense system of the skin contributing to the protection against the deleterious effects of UVA (9–11). Among the photo-protective agents with notable antioxidant activity, carotenoids are of major importance, being powerful natural $^1O_2$ quenchers (12). β-Carotene (βC) is widely used in supplements as a photoprotector, either alone or in combination with other antioxidants (13,14), based also on its

Abbreviations: AX, astaxanthin; βC, β-carotene; CAT, catalase; CX, canthaxanthin; DHR123, dihydrorhodamine; HDF, human dermal fibroblasts; HO-1, heme oxygenase-1; MDA, malondialdehyde; PI, propidium iodide; ROS, reactive oxygen species; SD, standard deviation; SOD, superoxide dismutase; TBARS, thiobarbituric acid reactive substances; THF, tetrahydrofuran.

provitamin A activity. The vitamin A derivative all-trans-retinoic acid, is the major biologically active retinoid, which however has limited use because of side effects. Optimised formulations of retinoic acid combined with other agents or as a precursor overcome side effects (15). Although it appears that important photoprotective actions can be attributed to carotenoids, there is an increasing concern that some of them may also display pro-oxidant side effects. As matter of the fact, when the photoprotective properties of βC were addressed, a number of conflicting results have emerged (16–22). Carotenoids other than βC, in particular, lycopene and several xanthophylls have been considered as substitutes for βC in photoprotective formulations (23–27). Apart from their distinct antioxidant properties, carotenoids exhibit several other biological functions such as provitamin A activity, modulation of gene expression and cell–cell communication (28,29). For evaluating the activity of carotenoids to modulate the UV-induced damages in skin, dermal fibroblasts are a suitable model system, being the primary target of long wave UV radiation, to which they respond through different pathways sensitive to oxidative signalling. Fibroblasts take up carotenes and related compounds at a significant extent (19,30). The aim of the present study was to investigate the photoprotective properties of astaxanthin (AX) compared to the congeners canthaxanthin (CX), and βC.

Materials and methods

Chemicals

Astaxanthin and CX were kindly provided by BASF (Ludwigshafen, Germany). β-Carotene was obtained from MP Biomedical (Asse-Relegem, Belgium). All the reagents and solvents were of the highest purity commercially available. Purity of carotenoids was determined by HPLC-DAD analysis and was ≥98% for all of them.

Carotenoid solutions

Stock solutions of the carotenoids were prepared in tetrahydrofuran (THF, purity > 99.9%, peroxide ≤ 0.01%) (Merck, Germany) in amber glass vials, in the dark, and at 4°C. The concentration of 10 mM of stock solutions was confirmed by spectrophotometry. The stock solutions were aliquoted and kept at −80°C until use. Dilution of the carotenoid solutions and cell treatment were performed under dim light.

Cell culture conditions and treatment

Human dermal fibroblasts (HDF) were obtained from child foreskin. Cells were cultured as monolayers in Dulbecco's modified Eagle's medium (DMEM) (Euroclone, Wetherby West York, UK), supplemented with 10% heat inactivated fetal bovine serum (FBS) (Hyclone, Logan, UT, USA), 2 mM L-glutamine, 100 μg/ml penicillin-streptomycin (all from GIBCO Life Technologies S.r.l., Milan, Italy) and maintained in a humidified atmosphere of 95% air and 5% CO_2 at 37°C. Cells were passaged every 3 days by trypsinisation and were used for experiments between passages 4 and 12. Cells were seeded in 6-cm^2-diameter culture dishes and pretreated with the carotenoids when the 90% confluence was reached. For treatment, carotenoid stock solutions were diluted to obtain final concentrations in the incubation medium in the range of 0.5–10 μM. Pretreatment was for 24 h prior to UVA irradiation.

UVA irradiation

The medium was withdrawn and cells were washed twice with isotonic solution and covered with phosphate-buffered saline (PBS). Irradiation was carried out at 30°C in a Bio-Sun irradiation apparatus (Vilbert Lourmat, Marnè-la-Vallèe, France) with maximum emission at 365 nm in the UVA spectral region (320–400 nm). The UVA dose rate was 3.9 ± 0.06 mW/cm^2, and the average irradiation time required to emit 10 J/cm^2 was 45 min. Following irradiation, PBS was replaced by fresh medium and cells were incubated until analysed. Control cells were treated identically but without UVA exposure. To assess the phototoxicity of UVA, HDF were irradiated with 0, 5, 10 and 15 J/cm^2 UVA, and the 3-(4,5-dimethylthiazol-2-yl)-2,5-diphenyltetrazolium bromide (MTT) toxicity assay (31) was performed 24 h after irradiation by measuring the optical density (OD) at 540 nm.

Cell death and apoptosis

Cell death and apoptosis were detected by the propidium iodide (PI) and annexin V staining methods (32). Briefly, HDF were harvested by trypsinisation and suspended in the staining buffer (10 mM HEPES/NaOH, pH 7.4, 140 mM NaCl, 2.5 mM $CaCl_2$). They were stained with FITC-labelled annexin V and PI, 1 μg/ml each, for 10 min and then analysed by FACSCalibur (Becton Dickinson, Mountain View, CA, USA) using Cell-Quest software for Macintosh.

Caspase-3 activity

Caspase-3 activity was assayed 12 h after irradiation using the CaspACE Assay System (Promega/Catalys, Wallisellen, Switzerland) with Ac-Asp-Glu-Val-Asp-p-nitroaniline (Ac-DEVD-pNA) as a substrate, according to the manufacturer's instructions. pNA is released upon cleavage and monitored spectrophotometrically at 405 nm. Caspase-3 activity was calculated using a calibration curve of pNA and normalised by the protein concentration of the cell extract. The caspase-3 activity was determined in three independent experiments in duplicate and expressed as μmol pNA/mg protein.

Reactive oxygen species – FACS analysis

Intracellular ROS were determined with dihydrorhodamine 123 (DHR123; Molecular Probes, Eugene, OR, USA) (33). Following exposure to 10 J/cm^2 UVA, cells were washed twice with PBS and incubated with 2.5 μM DHR123 at 37°C and 5% CO_2 in PBS containing 5 mM glucose. After 30-min incubation, cells were harvested by trypsinisation and centrifuged at 1200 rpm, then re-suspended in PBS with 5 mM glucose at a density of 2.5×10^5 cells/ml. The signal of green fluorescent rhodamine 123 (the oxidation product of DHR123) was measured by flow cytometry using FACSCalibur equipped with a 488 nm argon laser. A total of 10×10^3 cells from each sample were sorted; data were collected and processed with the Cell-Quest software. The median value of FL-1 channel of fluorescence was used to evaluate the intracellular content of rhodamine 123 as a measure of the ROS formation. The results are the mean of three experiments performed in duplicate.

Plasma membrane integrity

Fluorescein diacetate (FDA) (Fluka, AG, Switzerland) was used to assess UVA-induced membrane damage (34). Immediately after UVA exposure, cells were incubated with 1 μg/ml FDA in PBS at 37°C for 5 min. Control cells were kept in the dark. After rinsing with PBS, cells were harvested by trypsinisation and centrifuged at 1200 rpm, then suspended in PBS at a density of 2.5×10^5 cells/ml. The samples were kept on ice and immediately analysed using a FACSCalibur flow cytometer equipped with a 488-nm argon laser. A total of 10×10^3 cells from each sample were sorted, and Cell-Quest software was used to analyse the data. The results are reported as the mean of three experiments in duplicate.

Thiobarbituric acid reactive substances (TBARS)

The determination of TBARS was performed as described by Jentzsch et al. (35). Three hours after irradiation, cells were harvested and homogenised in the presence of butylated hydroxy toluene mixed with orthophosphoric acid and thiobarbituric acid. The reaction mixture was heated at 90°C for 45 min. Samples were put on ice to stop the reaction and extracted once with *n*-butanol. Absorption was read at 535 and 572 nm to normalise for the baseline absorption, with a Beckman DU-70 spectrophotometer (Beckman Coulter, Fullerton, CA, USA). TBARS equivalents were calculated using the difference in the absorption at the two wavelengths. Quantification was based on calibration curves using malondialdehyde (MDA) as a standard. The values, obtained as pmoles of MDA, were normalised for protein content determined with Bio-Rad protein assay (Bio-Rad, CA, USA). Three different determinations in duplicate were performed.

Activity of catalase and superoxide dismutase

Cells were lysed in PBS by repeated freezing and thawing, in the presence of protease inhibitors and centrifuged at 10 000 *g* for 10 min at 4°C. Enzyme activities were determined in the supernatant from cells harvested 3 h after irradiation. Catalase activity was determined spectrophotometrically measuring the loss of H_2O_2 at 240 nm (36); a standard curve was obtained with bovine CAT (Sigma-Aldrich, Milan, Italy). Superoxide dismutase activity was measured according to Spitz and Oberley (37). Superoxide generated by xanthine/xanthine–oxidase system was detected by monitoring the reduction of nitroblue tetrazolium (Sigma-Aldrich, St. Louis, MO, USA) at 560 nm. CAT and SOD activities were normalised for the protein content. Three assays were run with each supernatant, and experiments were repeated in duplicate.

RNA isolation and semiquantification of OH-1 mRNA levels by RT-PCR

Heme oxygenase-1 mRNA was analysed according to previously reported methods (38). The total RNA was extracted from the HDF using TRizol reagent (Invitrogen, Italy) according to the protocol of the manufacturer. Briefly, cells were homogenised in 1 ml TRIzol reagent and then extracted with 0.2 ml $CHCl_3$. Isopropanol (0.5 ml) was added to the aqueous phase. The RNA pellets were washed with ethanol and dissolved in RNase-free water. Total RNA quantity, purity, and absence of ribonuclease digestion were checked by measuring the ratio between absorbance at 260 and 280 nm and by electrophoresis on 1% agarose gel. The oligonucleotide primers for the PCR were: glyceraldehyde-3-phosphate dehydrogenase (GAPDH) sense: 5′-GCACCACCAACTGCTTAGC-3′ and antisense: 5′-TGCTCAGTG TAGCCCAGG-3′; for hemeoxygenase-1 (HO-1) sense 5′-CCAGCGGGCCAGCAACAA CGTGC-3′ and antisense 5′-AAGCCTTCAGTGCCCACGGTAAGG-3′. Reverse-transcriptase-PCR was carried out using 1 μg of total RNA. After denaturing in diethylpyrocarbonate-treated water (Promega Corporation, WI, USA) at 70°C for 10 min, RNA was reverse-transcribed into cDNA using ImProm-II^{TM} Reverse Transcriptase (1 μl per reaction; Promega) and 0.5 μg of oligo(dT) primers at 42°C for 60 min in a total volume of 20-μl ImProm-II^{TM} 5X reaction buffer (Promega) containing 1.5 mM $MgCl_2$, 0.5 mM dNTP and 20 U RNase inhibitor. Reverse transcriptase was inactivated at 70°C for 15 min and the RNA template was digested by RNase H at 37°C for 30 min. In each case, samples containing no reverse transcriptase (negative control) were added to exclude amplification from contaminating DNA. PCR reaction was carried out in the PCR Master Mix buffer (Promega) (25 μl total volume containing 1 μl cDNA, 20 pmol of oligonucleotide primers, 1 U Taq DNA

polymerase, 1.5 mM $MgCl_2$ and 0.2 mM dNTP). PCR amplification was performed with an iCycler thermal cycler (Bio-Rad, Milan, Italy). Each cycle consisted of 3 min at 94°C followed by 33 cycles at 94°C for 10 s, 60°C for 30 s, 72°C for 30 s, followed by a final cycle at 72°C for 5 min. PCR products were visualised by staining with ethidium bromide after the separation on 2% tris-acetate-ethylenediamine tretraacetic acid (TAE)-agarose gel. To semiquantitate the relative amounts of HO-1 mRNA, the band intensities were related densitometrically to the respective GAPDH PCR product of the same sample. Densitometric evaluation was performed using UVIDocMw software (Bio-Rad).

Western blot analysis of HO-1

Heme oxygenase-1 (HO-1) was determined as reported (38,39). Cell pellets were lysed in RIPA buffer supplemented with protease inhibitors. Protein content was determined with the Bio-Rad protein assay. Total cell lysate proteins (20 μg) were resolved in denaturing 12% polyacrylamide gel and transferred to a nitrocellulose membrane (Amersham Biosciences, NJ, USA). Protein transfer efficiency was checked with Ponceau S staining (Sigma-Aldrich, Milan, Italy). After washing with PBS, the membrane was blocked with 5% fat-free dry milk in PBS with 0.05% Tween-20 for 1 h at room temperature. After 30-min washing in PBS-0.05% Tween-20, the membrane was incubated with rabbit anti-HO-1 polyclonal antibody (Stressgen Bioreagents, MI, USA) 1:2000 in TBS-T-1% milk powder, overnight at 4°C. After washing with TBS-T, a secondary antibody goat anti-rabbit IgG-HRP 1:5000 (Santa Cruz Biotechnology Inc., CA, USA) was added for 1 h at RT. Bands were visualised by enhanced chemiluminescence (ECL) reagent (Santa Cruz Biotechnology Inc., CA, USA). β-Actin was used as a loading control.

HPLC analysis of carotenoids

HPLC analysis of carotenoids was performed as reported, with slight modification (40). All extractions and analytical procedures were operated in brown glass and in dim light. After lysis and centrifugation, proteins were determined in the supernatant with the Bio-Rad protein assay. The sample volume was brought to 1 ml with bidistilled water; 1 nmol lutein, as the internal standard, and 500 μl of ethanol were added. The mixtures were extracted three times with 3 ml of hexane; the organic layers were collected and the solvent was evaporated under a gentle stream of nitrogen. The dry residues were suspended in the HPLC eluent. HPLC was carried out on a Hewlett Packard 1090 (Agilent Technologies, CA, USA) liquid chromatograph fitted with Supelcosil LC-18 (25 cm × 4.6 mm) column preceded by guard column. Astaxanthin and CX were separated under isocratic condition with a mobile phase consisting of two eluents (a) hexane, and (b) acetonitrile/methanol 85/15 containing 50 mM ammonium acetate, in the A/B ratio 5/95, at a flow rate of 0.6 ml/min. For the elution of βC, the same eluents were used with an elution program starting from A/B 5/95 with a flow of 0.6 ml/min in the time range 0–9 min to A/B 10/90 with a flow rate of 0.8 ml/min in the time range 9–12 min and finally to A/B 12/88 with a flow rate of 1 ml/min from 18 to 35 min. Data were acquired by using a diode array detector set at 450 nm.

Statistical analysis

To assess significance, data sets were processed applying the Student's t test and differences were assumed to be statistically significant when $P \leq 0.05$.

Results

Modulation of UVA toxicity by carotenoids

The chemical structures of the carotenoids investigated are shown in Fig. 1. UVA irradiation dose-dependently increased cell toxicity in HDF, as detected by MTT assay at 24 h (Fig. 2a). HDF labelling with PI was 2.6% ± 0.6, and 3.4% ± 0.7 of the total cells, at 10 and 15 J UVA, respectively. The increased phototoxicity is at least partially associated with UVA-dependent apoptosis. Following UVA radiation, caspase-3 activity was increased at 12 h (Fig. 2b). Modest apoptosis was detected 24 h after UV irradiation, measuring Annexin V binding being 2.2% ± 0.4, and 3.1% ± 0.6 of the total cells, at 10 and 15 J UVA, respectively. Based on the above results, 10 J/cm^2 were selected as the working UVA dose for the experiments with AX, CX, and βC. HDF were loaded with the carotenoids at different concentrations 24 h prior to UVA irradiation. Twenty-four-hour post-irradiation, AX lowered UVA toxicity when preloaded at 5 and 10 μM, although differences were not significant (Fig. 3a). No effects on phototoxicity were observed when HDF were preloaded with CX. βC did not affect cell survival at levels of 0.5–2 μM. Concentrations of βC higher than 2 μM were phototoxic (Fig. 3a,b). Thus, further investigations with βC were performed at levels of

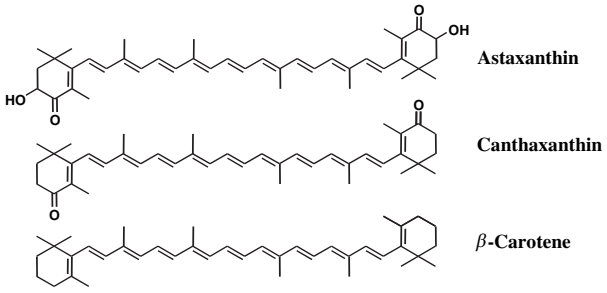

Figure 1. Structures of AX, CX, and βC.

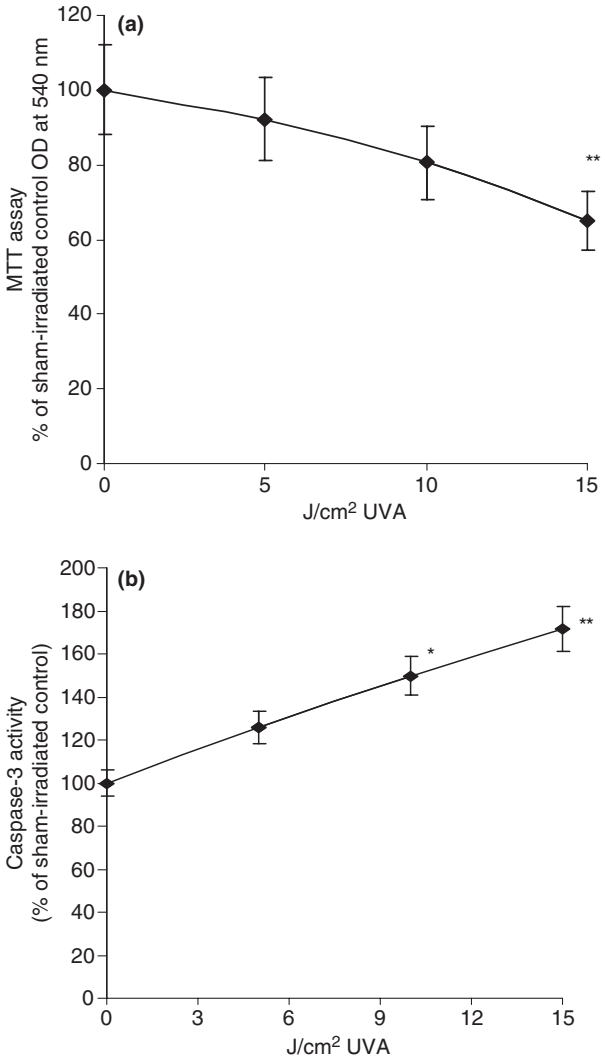

Figure 2. Phototoxicity (a) and caspase-3 activity (b) in HDF after exposure to 5–15 J/cm^2 UVA. Phototoxicity was assessed 24 h after irradiation by the MTT assay six times in triplicate. Caspase-3 activity was determined 12 h after irradiation, three times in duplicate; *$P < 0.05$; **$P < 0.005$, compared with the sham-irradiated control.

maximally 2 μM. The effects of carotenoids on UVA-induced cell toxicity were paralleled by modifications of caspase-3 activity and annexin V binding, which is used to detect early stages of apoptosis (Fig. 3c,d). Caspase-3 was decreased dose-dependently by AX, whereas effects on annexin V binding were detectable but not significant. Increasing levels of βC caused caspase-3 activity upregulation and aggravation of apoptosis, whereas CX had no significant effects (Fig. 3c,d).

Cellular uptake and photostability of carotenoids in fibroblasts

Cellular uptake of carotenoids was measured after 24 h of incubation. Carotenoids were delivered to the cells as a suspension obtained by thoroughly mixing stock solutions of the compounds dissolved in THF with complete medium to obtain a final concentration of 10 μM for AX and CX, and of 2 μM for βC. None of the carotenoids investigated were detected in the vehicle-treated cells. HPLC analyses revealed that the carotenoids were taken up with a different degree. AX was uploaded more efficiently than the other two carotenoids; CX and βC reached comparable intracellular levels, albeit βC was supplied at a lower level (Table 1). The cell content of carotenoids following supplementation was comparable with those previously reported (40,41). The supplementation time with CX was prolonged up to 96 h in order to achieve a higher cellular uptake at which investigate the effects on the modification of some of the parameters of cell oxidative damage. CX was time-dependently accumulated in HDF between 24 and 72 h, with the latter time point corresponding to the highest intracellular concentration reached (228 ± 42 nmol/mg protein).The intracellular levels of CX declined in the following hours reaching a concentration of 175 ± 16 nmol/mg protein at 96 h. To verify the photostability of the compounds, the concentrations of AX, CX, and βC were measured after exposure of loaded cells to 10 J/cm^2 UVA. No significant change in AX levels was found comparing pre- and post-irradiation cell extracts (Table 1). After photoirradiation, CX presented a slight but significant decrease of the initial level reached at 24 h incubation (Table 1), and a more pronounced photodegradation following 72 h upload, being 160 ± 22 nmol/mg protein, the concentration of CX recovered after UVA. In contrast, βC was almost completely decomposed under the same conditions (Table 1).

Modulation of UVA-induced ROS generation by carotenoids

Reactive oxygen species generation is a well-established effect of UVA irradiation. To measure ROS, the relative amount of rhodamine 123, produced by oxidation of DHR123, was determined by flow cytometry. UVA (10 J/cm^2) led to a significant ROS elevation (median of fluorescence 117 ± 10, $P < 0.005$) (Fig. 4a), which was decreased by 30% and 50% in cells pretreated for 24 h with AX at 5 μM (median of fluorescence 81 ± 6, $P < 0.05$) and 10 μM (median of fluorescence 57 ± 8, $P < 0.001$), respectively. Treatment for 24 h with CX or βC showed no effect on UVA-induced ROS formation. To define whether the extent of uptake could influence the ROS scavenging capacity of CX, FACS analysis were performed at prolonged preincubation times. In spite of the increased uptake of CX, no effects on the UVA-induced ROS were observed at any of the pretreatment times (data not reported).

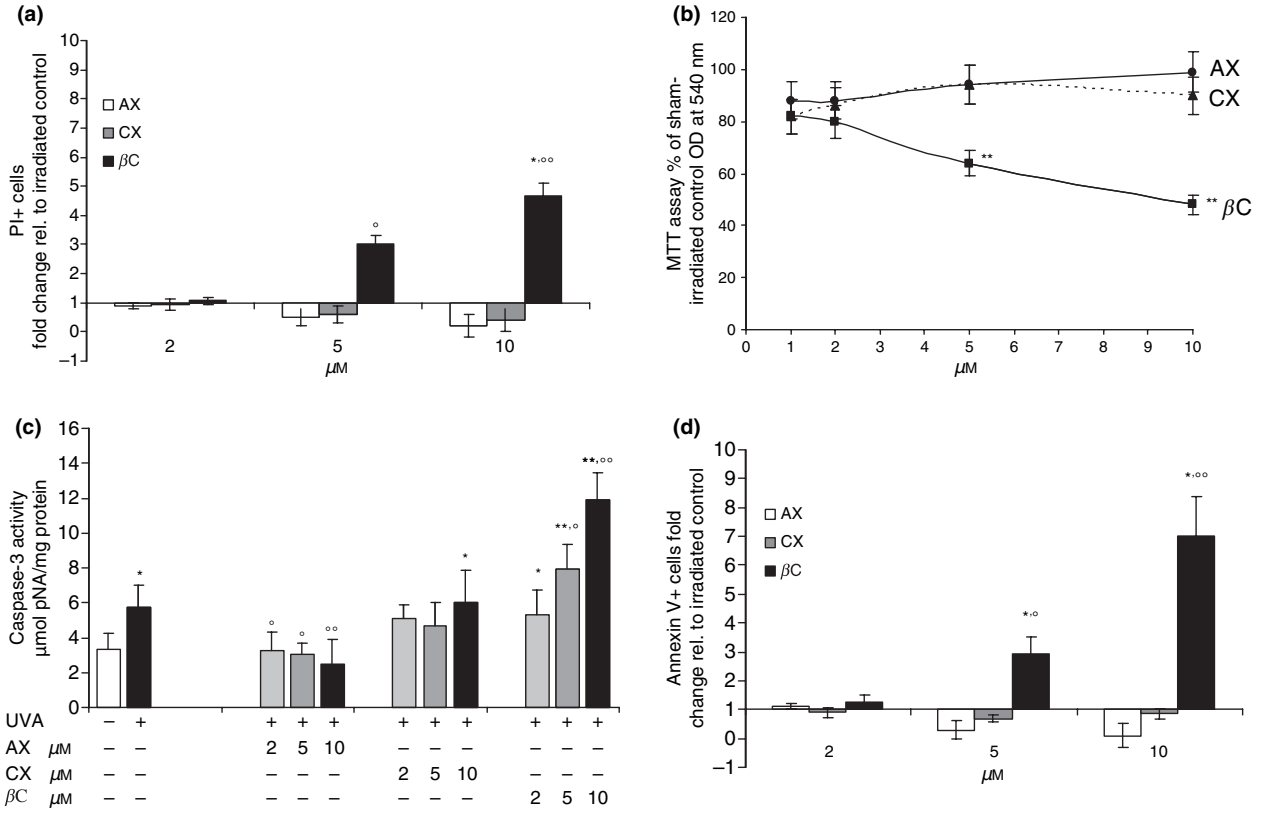

Figure 3. Cell survival and phototoxicity of AX, CX, and βC at 10 J/cm^2 UVA assessed by PI staining method (a) and MTT assay (b) at 24 h after irradiation. Effects of carotenoids on the UVA-induced activation of caspase-3 (c) and apoptosis (d), which was detected by annexin V staining, were analysed 12 and 24 h after irradiation, respectively. For experimental conditions refer to Fig. 2 and the experimental section. *$P < 0.05$ and **$P < 0.005$, compared with the corresponding sham-irradiated control; °$P < 0.05$ and °°$P < 0.005$ compared with the irradiated control HDF pretreated with the vehicle only. MTT assay was performed six times in triplicate, whereas PI and Annexin V staining, as well as caspase-3 activity were determined three times in duplicate.

Effects of carotenoids on UVA-induced changes of membrane integrity and TBARS formation

UVA irradiation induced a substantial decline of plasma membrane integrity as measured by the decrease in the FDA uptake/retention ($P < 0.01$), directly after UVA exposure (Fig. 4b). Pretreatment with 10 μM AX prevented UVA-induced leakage of fluorescein ($P < 0.05$), whereas leakage was more pronounced when HDF were preincubated with 2 μM βC. In contrast, CX had no effect on the membrane perturbation caused by UVA.

Preincubation of fibroblasts with carotenoids did not influence the basal TBARS levels (Table 1). Upon UVA

Table 1. Effects of 24 h AX, CX, and βC on formation of TBARS, activities of CAT and SOD and carotenoids levels in HDF, with and without UVA irradiation

	UVA (J/cm$_2$)	TBARS (nmol MDA/mg protein)	CAT activity (U/mg protein)	SOD activity (U/mg protein)	Carotenoid levels (nmol/mg protein)
Control (THF 0.1%)	0	3.1 ± 0.3	7.0 ± 0.6	114 ± 5.6	n.d.
	10	4.5 ± 0.6*	5.1 ± 0.5*	86.5 ± 4.3*	n.d.
Astaxanthin (10 μM)	0	2.9 ± 0.4	6.9 ± 0.6	105 ± 8.0	245 ± 33
	10	3.1 ± 0.3°	6.7 ± 0.4°	109 ± 5.0°	244 ± 38
Canthaxanthin (10 μM)	0	3.1 ± 0.6	6.4 ± 0.8	102 ± 9.7	65.4 ± 14
	10	4.4 ± 0.2*	5.2 ± 0.6	91.6 ± 6.3	58.9 ± 16*
β-Carotene (2 μM)	0	2.9 ± 0.4	7.1 ± 0.5	112 ± 6.6	22.2 ± 4.6
	10	5.2 ± 0.8*°	6.0 ± 0.5	105 ± 5.8°	0.98 ± 0.14**

Values are mean ± SD of three experiments in duplicate. *$P < 0.05$ versus sham-irradiated control; °$P < 0.05$ versus irradiated HDF pretreated with the vehicle only.

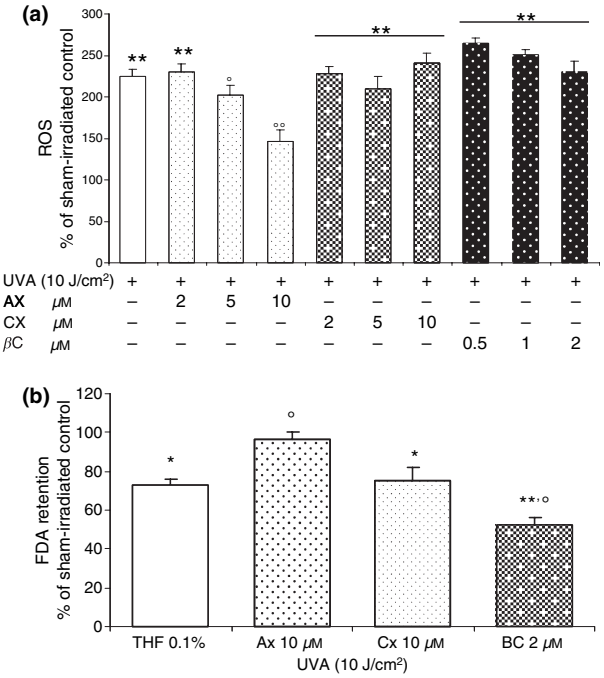

Figure 4. Effects of AX, CX, and βC on UVA-induced formation of ROS (a) and changes of plasma membrane integrity (b) in HDF. Cells were pretreated for 24 h with 10 μM AX and CX, and 2 μM βC and irradiated with 10 J/cm^2 UVA. ROS formation was determined following oxidation of DHR123 to the fluorescent rhodamine 123 using FACS analysis. The reported values represent the mean ± SD of three experiments performed in duplicate. °$P < 0.05$ and °°$P < 0.005$ compared with irradiated HDF pretreated with the vehicle only. Plasma membrane integrity was determined by FACS analysis measuring the retained fluorescence of FDA in UVA-irradiated and non-irradiated HDF. The values are expressed as a percentage of fluorescence compared with non-irradiated control cells. The results are reported as mean ± SD of three experiments in duplicate. *$P < 0.05$ compared with the non-irradiated control; °$P < 0.05$ compared with irradiated HDF pretreated with the vehicle only.

irradiation, TBARS levels were increased by 40% ($P < 0.05$) in control cells. AX inhibited the UVA-induced formation of TBARS ($P < 0.05$). In comparison to the irradiated control cells (THF 0.1%), TBARS formation was lowered to about 70%. After 24-h pretreatment with CX, no change of TBARS levels was observed when compared with the irradiated control. By increasing upload of CX, no effects on the TBARS levels were recorded, even at a cellular uptake comparable to that of AX (data not shown). In contrast, the amount of TBARS was elevated in irradiated HDF loaded with 2 μM βC and exposed to 10 J/cm^2 UVA indicating a pro-oxidant effect of this compound under the present conditions (Table 1).

Effects of carotenoids on UVA-induced inhibition of CAT and SOD activity

To evaluate whether carotenoids influenced UVA-dependent inhibition of the antioxidant enzymes CAT and SOD, enzymatic activities were analysed 3 h after UVA irradiation in the presence and absence of the compounds (Table 1). UVA (10 J/cm^2) led to a significant decrease of CAT activity. This decrease in CAT activity was significantly lower at 10 μM AX and less pronounced in the presence of 2 μM βC. No change was found with 10 μM CX. After fibroblasts had been exposed to UVA, a significant decrease of SOD activity was also detected. Supplementing HDF with AX or βC counteracted this effect, whereas CX was ineffective.

Effects of carotenoids on UVA-stimulated expression of HO-1

In order to investigate the role of AX in the UVA-induced activation of genes sensitive to oxidative stress, compared with the congeners, we evaluated the induction of HO-1 at the mRNA and protein levels, in HDF preloaded with 10 μM AX and CX or 2 μM βC for 24 h and irradiated with 10 J/cm^2 UVA light (Fig. 5). Levels of HO-1 mRNA were measured 3 h after UVA exposure, whereas the protein expression was evaluated 12 h after irradiation. UVA-irradiated control cells showed a 70% induction of mRNA when compared with basal levels ($P < 0.05$). Pretreatment with AX lowered the UVA-mediated induction of HO-1 mRNA, whereas CX and βC enhanced these effects by 98% ($P < 0.05$), and 300% ($P < 0.01$) when compared with sham-irradiated controls. In the UVA-exposed control cells, also a significant increase of HO-1 protein levels (50%, $P < 0.01$) was detected. In non-irradiated cells preincubated with CX, and βC, a moderate induction of HO-1 expression was observed. AX clearly prevented UVA-induced upregulation of HO-1 expression at 12 h ($P < 0.005$), whereas irradiation of HDF preloaded with CX led to a significant increase in HO-1 protein levels ($P < 0.01$) as for βC.

Discussion

In the present study, we evaluated the photoprotective properties of AX in comparison to CX and βC in HDF. A 'physiological' dose of UVA was applied, roughly corresponding to a UV dose accumulated within 1–2 h on a sunny day at latitude of 35°N (42). An early effect of skin exposure to UVA is a rise in ROS, which are normally scavenged by an efficient antioxidant defense system, consisting of enzymes and low-molecular weight compounds. However, antioxidant enzymes are themselves targets for oxidative modifications triggered by UVA. The impairment of CAT activity caused by UVA is ascribed to the direct effects of radiation on photosensitive sites of the protein and to indirect actions mediated by the release of singlet oxygen and other ROS (43). It is worth mentioning that the investigated carotenoids are poor filters in the used

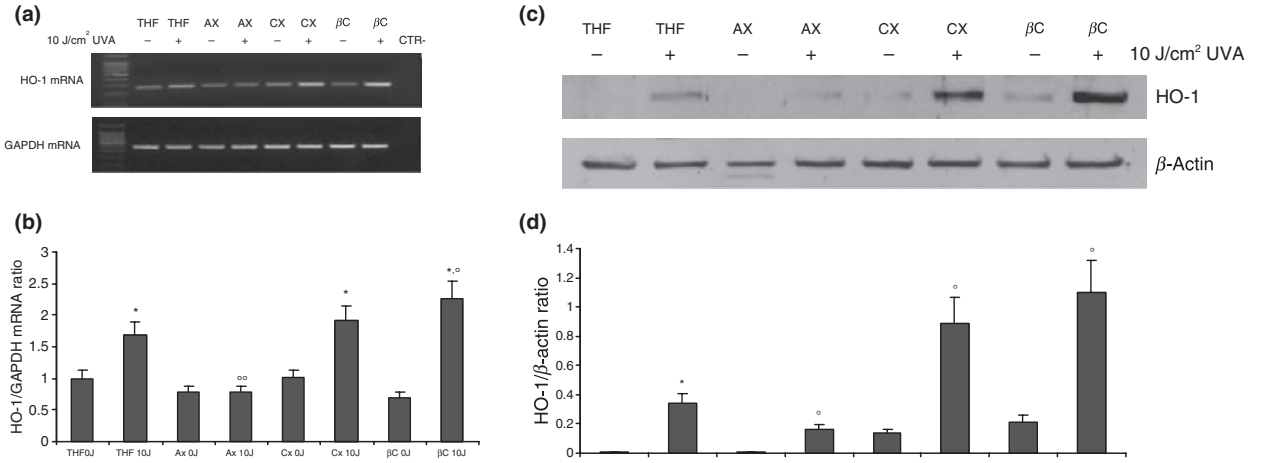

Figure 5. Northern and Western blot analysis of HO-1 mRNA in HDF treated for 24 h with 10 μM AX and CX, as well as 2 μM βC. Cells were harvested 3 and 12 h after irradiation and analysed for HO-1 mRNA and protein expression. Northern blot and Western blot representative of three experiments, are shown in panel (a) and (c), respectively. β-Actin was used as the loading control for the HO-1 protein detection, whereas HO-1 mRNA levels were normalised over GAPDH mRNA. The relative densities shown represent the mean of three Western blots (b) and three RT-PCR (d) experiments. $^*P < 0.05$ versus sham-irradiated control; $^\circ P < 0.05$ versus irradiated HDF pretreated with the vehicle only.

UVA range (44). AX abrogated the UVA-induced CAT inhibition. βC, which is an efficient $^1O_2$-quencher, displayed a slight photoprotective effect towards the impairment of CAT activity. No effects on the impairment of CAT were exerted by CX. Similarly, the inhibition of SOD by UVA was counteracted by AX and βC, but not by CX. One can speculate that βC interferes with the UVA-induced inhibition of SOD activity by a specific mechanism, possibly related to a selective scavenging action exerted towards individual free radical species (2). The greater ROS scavenging activity exhibited by AX when compared with the congener CX can be partly ascribed to the different structural features of the two compounds. Because βC was phototoxic at levels higher than 2 μM, as demonstrated by the lowered cell viability following UVA irradiation, higher concentrations were not investigated. Determining the uptake of AX, CX, and βC by HDF at 24 h, we found that AX was absorbed at levels ca. fourfold higher than CX, in agreement with reported studies performed either *in vitro* or *in vivo* comparing uptake of carotenes and xanthophylls (41,45). βC had an intermediate uptake level, provided that it was supplied fivefold less concentrated than CX. Prolongation of loading time with CX led to a higher accumulation of this compound, which, however, was ineffective in preventing cell photo-damages. ROS elevation and depletion of the antioxidant defense system are involved in the UVA-induced apoptosis, which occurs via caspases activation (22). Little is known about apoptotic control of chronological and photo-induced ageing of skin *in vivo*. Dermal fibroblasts in culture are widely used to model ageing, which is induced by applying apoptotic stimuli (46). Challenges with sublethal oxidative stresses, such as H_2O_2 or UV, result in the development of senescent-like growth arrest, in which caspases preside to cell degradation (47). The activity of caspase-3 was correlated with the UVA doses administered and with the levels of ROS (data not shown). When carotenoids were investigated for their effects on the UVA-induced activation of caspase-3, only AX efficiently abrogated the apoptotic response to UVA. The broad protection offered by AX towards the elevation of ROS and the oxidative damages mediated by UVA was probably involved in the prevention of the caspase-3 activation. CX, which was ineffective in opposing the elevation of ROS, did not interfere with the mechanism of induction of caspase-3 by UVA. In contrast, the pro-oxidant effects of βC under UVA exposure may be responsible for the enhanced apoptotic response to UVA. Plasma membrane stability of HDF was affected immediately after UVA exposure, according to established effects of UVA on membrane lipid peroxidation in fibroblasts (48,49). The diminished retention of FDA following UVA reflects a structural modification of the membrane that might initiate an intracellular stress response. The membrane perturbation detected by FDA residual fluorescence was paralleled by an increase in TBARS. Changes in both parameters show that AX effectively protects the plasma membrane against oxidative damage and loss of function. It has been suggested that oxo-carotenoids like AX and CX, are more effective in preventing lipid peroxidation than carotenes (50,51). We cannot exclude that part of the enhancing effects of βC on the UVA-induced damages are ascribable to its breakdown photoproducts, which might have formed under the given conditions, as βC-treated cultures were irradiated not at optimal loading levels. Carotenoids display a range of stability when exposed to various physical and chemical oxidative treatments. Pro-oxidant effects of βC have been

shown in different experimental conditions (52,53), and there is evidence that pro-apoptotic activities of βC are mediated by its oxidised species (54).

Astaxanthin behaved distinctly under photo-oxidative conditions. Indeed, AX, rather photostable, offered photoprotection. To better understand the modulating effects of AX on the UVA-induced response in fibroblasts, we investigated also the expression of HO-1, which is a marker of oxidative stress and a-regulatory mechanism involved in the modulation of the inflammatory responses and cell adaptation against oxidative damage (55). There is an evidence for a role of photochemically generated $^1O_2$ as an effector species of UVA in upregulating HO-1 expression (39). HO-1 gene expression is regulated via various stress-sensitive transcription factors, including Nrf2, which binds to antioxidant response elements in the promoter regions of enzymes of the detoxifying metabolism (56). Interestingly, AX prevented the upregulation of HO-1 by UVA. On the contrary, we observed a marked enhancement of UVA-induced HO-1 mRNA and protein expression by CX and βC indicating a role of AX in inhibition of UVA-induced ROS formation, which is upstream of the other parameters of oxidative damage studied. Similarly, the elevated lipid photo-oxidation in fibroblasts might be responsible for the enhancement of UVA-induced HO-1 expression by βC (57,58). In fact, a signalling role triggered by the release of diacylglycerol, as well as of arachidonic acid and its products of advanced oxidation, such as MDA and 4-hydroxynonenal, has been demonstrated in the induction mechanisms of HO-1 by UVA (59). Additionally, βC and CX may decompose under pro-oxidative conditions to yield reactive intermediates. The presence of antioxidants possibly preventing βC decomposition under oxidising conditions may be responsible for the abrogation of UVR-induced HO-1 upregulation by βC observed in other studies (39).

Our study highlights the different ability of the three carotenoids to counteract photo-oxidative damage, demonstrating a superior effect of AX in reducing or abrogating the UVA-induced stress responses, aiding the maintenance of a favourable redox status in UVA-irradiated fibroblasts in culture. The two hydroxyketo end-groups may be responsible for the greater antioxidant capacity of AX over its congeners. AX efficiently counteracts the depletion of antioxidant enzymes, the derangement of plasma membrane, and the apoptotic process when fibroblasts are irradiated, providing an effective and comprehensive protection by abrogating the enhancement of ROS, as it is an early event of UVA exposure. CX, which was ineffective towards the direct cell damage delivered by UVA, including the ROS elevation, might however exert a beneficial action through the induction of phase II detoxifying enzymes, as demonstrated by the upregulation of the HO-1 gene. In contrast, βC showed either pro- or antioxidant properties at concentrations lower than the two congeners. Human studies are relatively consistently showing UV-protective effects of βC. A recent meta-analysis of controlled clinical studies has shown overall protective effects of βC supplementation against sunburn, which is a skin reaction to the shorter wavelengths UVB (60). From the results of our study we can infer that AX, by supplying skin cells with a broad photoprotection, offers a safe measure for the prevention of a variety of UVA-induced skin damage, mainly mediated by ROS.

Acknowledgements

The present study was supported by the Deutsche Forschungsgemeinschaft (Bonn, Germany; Sonderforschungsbereich 663, B1). H.S. is a Fellow of the National Foundation for Cancer Research (NFCR), Bethesda, MD. E.C. was funded by the Italian Ministry of Health.

References

1 Ichihashi M, Ueda M, Budiyanto A *et al.* UV-induced skin damage. Toxicology 2003: **189**: 21–39.
2 Dalle Carbonare M, Pathak M A. Skin photosensitizing agents and the role of reactive oxygen species in photoaging. J Photochem Photobiol B 1992: **14**: 105–124.
3 Wondrak G T, Jacobson M K, Jacobson E L. Endogenous UVA-photosensitizers: mediators of skin photodamage and novel targets for skin photoprotection. Photochem Photobiol Sci 2006: **5**: 215–237.
4 Berneburg M, Grether-Beck S, Kurten V *et al.* Singlet oxygen mediates the UVA-induced generation of the photoaging-associated mitochondrial common deletion. J Biol Chem 1999: **2742**: 15345–15349.
5 Wlaschek M, Briviba K, Stricklin G P, Sies H, Scharffetter-Kochanek K. Singlet oxygen may mediate the ultraviolet A-induced synthesis of interstitial collagenase. J Invest Dermatol 1995: **104**: 194–198.
6 Scharffetter-Kochanek K, Wlaschek M, Brenneisen P *et al.* UV-induced reactive oxygen species in photocarcinogenesis and photoaging. Biol Chem 1997: **378**: 1247–1257.
7 Fisher G J, Datta S C, Talwar H S *et al.* Molecular basis of sun-induced premature aging and retinoid antagonism. Nature 1996: **379**: 335–339.
8 Shindo Y, Witt E, Han D, Packer L. Dose-response effects of acute ultraviolet irradiation on antioxidants and molecular markers of oxidation in murine epidermis and dermis. J Invest Dermatol 1994: **102**: 470–475.
9 Steenvoorden D P, van Henegouwen G M. The use of endogenous antioxidants to improve photoprotection. J Photochem Photobiol B 1997: **41**: 1–10.
10 Stahl W, Heinrich U, Wiseman S, Eichler O, Sies H, Tronnier H. Dietary tomato paste protects against ultraviolet light-induced erythema in humans. J Nutr 2001: **131**: 1449–1451.
11 Jańczyk A, Garcia-Lopez M A, Fernandez-Peñas P *et al.* A Polypodium leucotomos extract inhibits solar-simulated radiation-induced TNF-alpha and iNOS expression, transcriptional activation and apoptosis. Exp Dermatol 2007: **16**: 823–829.
12 Di Mascio P, Kaiser S, Sies H. Lycopene as the most efficient biological carotenoid singlet oxygen quencher. Arch Biochem Biophys 1989: **274**: 532–538.
13 Sies H, Stahl W. Nutritional protection against skin damage from sunlight. Annu Rev Nutr 2004: **24**: 173–200.
14 Greul A K, Grundmann J U, Heinrich F *et al.* Photoprotection of UV-irradiated human skin: an antioxidative combination of vitamins E and C, carotenoids, selenium and proanthocyanidins. Skin Pharmacol Appl Skin Physiol 2002: **15**: 307–315.
15 Jacobson M K, Kim H, Coyle W R *et al.* Effect of myristyl nicotinate on retinoic acid therapy for facial photodamage. Exp Dermatol 2007: **16**: 927–935.
16 Burton G W, Ingold K U. beta-Carotene: an unusual type of lipid antioxidant. Science 1984: **224**: 569–573.
17 Biesalski H K, Obermüller-Jevic U C. UV light, beta-carotene and human skin-beneficial and potentially harmful effects. Arch Biochem Biophys 2001: **389**: 1–6.
18 Fuchs J. Potentials and limitations of the natural antioxidants RRR-alpha-tocopherol, L-ascorbic acid and beta-carotene in cutaneous photoprotection. Free Radic Biol Med 1998: **25**: 848–873.
19 Eicker J, Kürten V, Wild S *et al.* Betacarotene supplementation protects from photoaging-associated mitochondrial DNA mutation. Photochem Photobiol Sci 2003: **2**: 655–659.

20 Césarini J P, Michel L, Maurette J M, Adhoute H, Béjot M. Immediate effects of UV radiation on the skin: modification by an antioxidant complex containing carotenoids. Photodermatol Photoimmunol Photomed 2003: **19**: 182–189.

21 Swindells K, Rhodes L E. Influence of oral antioxidants on ultraviolet radiation-induced skin damage in humans. Photodermatol Photoimmunol Photomed 2004: **20**: 297–304.

22 Wertz K, Hunziker P B, Seifert N *et al.* beta-Carotene interferes with ultraviolet light A-induced gene expression by multiple pathways. J Invest Dermatol 2005: **124**: 428–434.

23 Palozza P, Krinsky N I. Astaxanthin and canthaxanthin are potent antioxidants in a membrane model. Arch Biochem Biophys 1992: **297**: 291–295.

24 Mathews-Roth M M. Carotenoids in erythropoietic protoporphyria and other photosensitivity diseases. Ann N Y Acad Sci 1993: **691**: 127–138.

25 Kennedy A R, Krinsky N I. Effects of retinoids, beta-carotene, and canthaxanthin on UV- and X-ray-induced transformation of C3H10T1/2 cells in vitro. Nutr Cancer 1994: **22**: 219–232.

26 Savouré N, Briand G, Amory-Touz M C, Combre A, Maudet M, Nicol M. Vitamin A status and metabolism of cutaneous polyamines in the hairless mouse after UV irradiation: action of beta-carotene and astaxanthin. Int J Vitam Nutr Res 1995: **65**: 79–86.

27 Eichler O, Sies H, Stahl W. Divergent optimum levels of lycopene, beta-carotene and lutein protecting against UVB irradiation in human fibroblaststst. Photochem Photobiol 2002: **75**: 503–506.

28 Zhang L X, Cooney R V, Bertram J S. Carotenoids up-regulate connexin43 gene expression independent of their provitamin A or antioxidant properties. Cancer Res 1992: **52**: 5707–5712.

29 Stahl W, von Laar J, Martin H D, Emmerich T, Sies H. Stimulation of gap junctional communication: comparison of acyclo-retinoic acid and lycopene. Arch Biochem Biophys 2000: **373**: 271–274.

30 Offord E A, Gautier J C, Avanti O *et al.* Photoprotective potential of lycopene, beta-carotene, vitamin E, vitamin C and carnosic acid in UVA-irradiated human skin fibroblasts. Free Radic Biol Med 2002: **32**: 1293–1303.

31 Mosmann T. Rapid colorimetric assay for cellular growth and survival: application to proliferation and cytotoxicity assays. J Immunol Methods 1983: **652**: 55–63.

32 Ohshima S. Apoptosis and necrosis in senescent human fibroblasts. Ann N Y Acad Sci 2006: **1067**: 228–234.

33 Didier C, Kerblat I, Drouet C, Favier A, Beani J C, Richard M J. Induction of thioredoxin by ultraviolet-A radiation prevents oxidative-mediated cell death in human skin fibroblasts. Free Radic Biol Med 2001: **31**: 585–598.

34 Larsson P, Andersson E, Johansson U, Öllinger K, Rosdahl I. Ultraviolet A and B affect human melanocytes and keratinocytes differently. A study of oxidative alterations and apoptosis. Exp Dermatol 2005: **14**: 117–123.

35 Jentzsch A M, Bachmann H, Fürst P, Biesalski H K. Improved analysis of malondialdehyde in human body fluids. Free Radic Biol Med 1996: **20**: 251–256.

36 Claiborne A. Catalase activity. In: Greenwald R A, ed. Handbook of Methods for Oxygen Radical Research. Boca Raton: CRC Press, 1985: 283–284.

37 Spitz D R, Oberley L W. An assay for superoxide dismutase activity in mammalian tissue homogenates. Anal Biochem 1989: **179**: 8–18.

38 Keyse S M, Tyrrell R M. Heme oxygenase is the major 32-kDa stress protein induced in human skin fibroblasts by UVA radiation, hydrogen peroxide, and sodium arsenite. Proc Natl Acad Sci U S A 1989: **86**: 99–103.

39 Trekli M C, Riss G, Goralczyk R, Tyrrell R M. Beta-carotene suppresses UVA-induced HO-1 gene expression in cultured FEK4. Free Radic Biol Med 2003: **34**: 456–464.

40 Steghens J-P, van Kappel A L, Riboli E, Collombel C. Simultaneous measurement of seven carotenoids, retinol and α-tocopherol in serum by high-performance liquid chromatography. J Chromatogr B 1997: **694**: 71–81.

41 O'Sullivan L, Ryan L, O'Brien N. Comparison of the uptake and secretion of carotene and xanthophyll carotenoids by Caco-2 intestinal cells. Br J Nutr 2007: **98**: 38–44.

42 Godar D E. UV doses worldwide. Photochem Photobiol 2005: **81**: 736–749.

43 Maresca V, Flori E, Briganti S *et al.* UVA-induced modification of catalase charge properties in the epidermis is correlated with the skin phototype. J Invest Dermatol 2006: **126**: 182–190.

44 Miller N J, Sampson J, Candeias L P, Bramley P M, Rice-Evans C A. Antioxidant activities of carotenes and xanthophylls. FEBS Lett 1996: **384**: 240–242.

45 Chew B P, Park J S, Wong M W, Wong T S. A comparison of the anticancer activities of dietary beta-carotene, canthaxanthin and astaxanthin in mice in vivo. Anticancer Res 1999: **19**: 1849–1853.

46 Ohshima S. Apoptosis in stress-induced and spontaneously senescent human fibroblasts. Biochem Biophys Res Commun 2004: **324**: 241–246.

47 Thornberry N A, Lazebnik Y. Caspases: enemies within. Science 1998: **281**: 1312–1316.

48 Gaboriau F, Morlière P, Marquis I, Moysan A, Gèze M, Dubertret L. Membrane damage induced in cultured human skin fibroblasts by UVA irradiation. Photochem Photobiol 1993: **58**: 515–520.

49 Woodall A A, Britton G, Jackson M J. Carotenoids and protection of phospholipids in solution or in liposomes against oxidation by peroxyl radicals: relationship between carotenoid structure and protective ability. Biochim Biophys Acta 1997: **1336**: 575–586.

50 Woodall A A, Lee S W, Weesie R J, Jackson M J, Britton G. Oxidation of carotenoids by free radicals: relationship between structure and reactivity. Biochim Biophys Acta 1997: **1336**: 33–42.

51 Lim B P, Nagao A, Terao J, Tanaka K, Suzuki T, Takama K. Antioxidant activity of xanthophylls on peroxyl radical-mediated phospholipids peroxidation. Biochim Biophys Acta 1992: **1126**: 178–184.

52 Young A J, Lowe G M. Antioxidant and prooxidant properties of carotenoids. Arch Biochem Biophys 2001: **385**: 20–27.

53 El-Agamey A, Lowe G M, McGarvey D J *et al.* Carotenoid radical chemistry and antioxidant/pro-oxidant properties. Arch Biochem Biophys 2004: **430**: 37–48.

54 Palozza P, Calviello G, Serini S *et al.* beta-carotene at high concentrations induces apoptosis by enhancing oxy-radical production in human adenocarcinoma cells. Free Radic Biol Med 2001: **30**: 1000–1007.

55 Applegate L A, Luscher P, Tyrrell R M. Induction of heme oxygenase: a general response to oxidant stress in cultured mammalian cells. Cancer Res 1991: **51**: 974–978.

56 Alam J, Stewart D, Touchard C, Boinapally S, Choi A M, Cook J L. Nrf2, a Cap'n'Collar transcription factor, regulates induction of the heme oxygenase-1 gene. J Biol Chem 1999: **274**: 26071–26078.

57 Obermüller-Jevic U C, Francz P I, Frank J, Flaccus A, Biesalski H K. Enhancement of the UVA induction of haem oxygenase-1 expression by beta-carotene in human skin fibroblasts. FEBS Lett 1999: **460**: 212–216.

58 Obermüller-Jevic U C, Schlegel B, Flaccus A, Biesalski H K. The effect of beta-carotene on the expression of interleukin-6 and heme oxygenase-1 in UV-irradiated human skin fibroblasts in vitro. FEBS Lett 2001: **509**: 186–190.

59 Basu-Modak S, Lüscher P, Tyrrell R M. Lipid metabolite involvement in the activation of the human heme oxygenase-1 gene. Free Radic Biol Med 1996: **20**: 887–897.

60 Köpcke W, Krutmann J. Protection from Sunburn with beta-Carotene-A Meta-analysis. Photochem Photobiol 2008: **84**: 284–288.